**Neuroscience**

**The Journal of Physiology**

SYMPOSIUM REVIEW

Modelling effects on grid cells of sensory input during self-motion

Florian Raudies, James R. Hinman and Michael E. Hasselmo

Center for Systems Neuroscience, Centre for Memory and Brain, Department of Psychological and Brain Sciences and Graduate Program for Neuroscience, Boston University, 2 Cummington Mall, Boston, MA 02215, USA
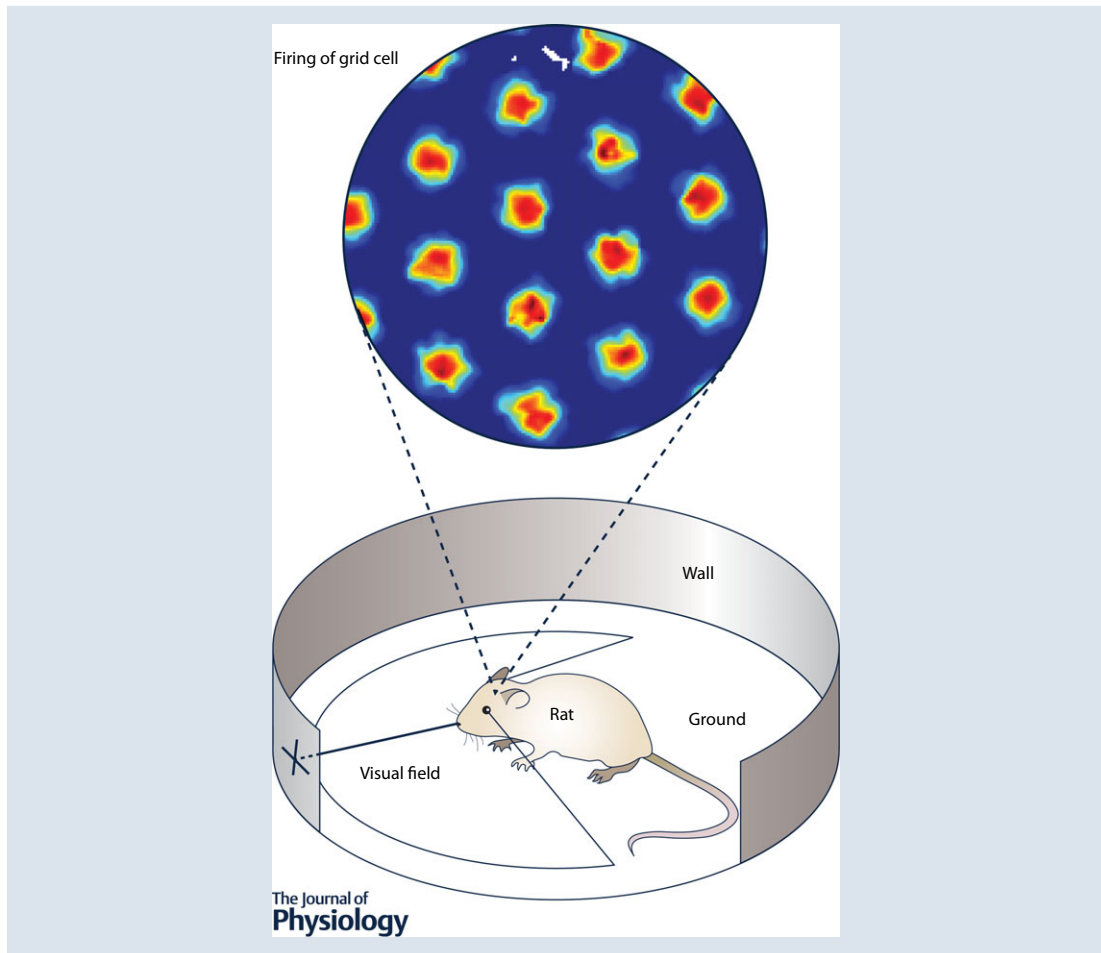
Florian Raudies obtained his PhD in Computer Science (summa cum laude) from the University of Ulm, Germany, working with Prof. Heiko Neumann. He worked as a post-doctoral fellow and Research Assistant Professor at Boston University in the Department of Psychological and Brain Sciences and the Centre for Computational Neuroscience and Neural Technology before taking his current position as a Research Engineer at Hewlett Packard Labs. **James R. Hinman** obtained his PhD in Psychology from the University of Connecticut working with Prof. James Chrobak and is currently a post-doctoral fellow at Boston University. **Michael E. Hasselmo** is a Professor in the Department of Psychological and Brain Sciences and the Director of the Center for Systems Neuroscience at Boston University. He is principal investigator on two NIMH R01 grants and an ONR MURI award.
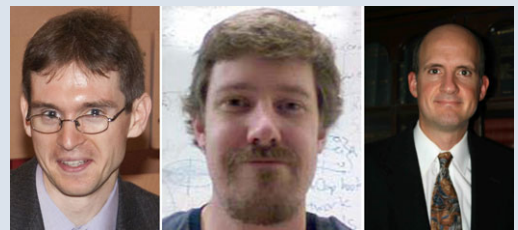
This review was presented at the symposium "Spatial Computation: from neural circuits to robot navigation", which took place at the University of Edinburgh, on 11 April 2015.

Abstract The neural coding of spatial location for memory function may involve grid cells in the medial entorhinal cortex, but the mechanism of generating the spatial responses of grid cells remains unclear. This review describes some current theories and experimental data concerning the role of sensory input in generating the regular spatial firing patterns of grid cells, and changes in grid cell firing fields with movement of environmental barriers. As described here, the influence of visual features on spatial firing could involve either computations of self-motion based on optic flow, or computations of absolute position based on the angle and distance of static visual cues. Due to anatomical selectivity of retinotopic processing, the sensory features on the walls of an environment may have a stronger effect on ventral grid cells that have wider spaced firing fields, whereas the sensory features on the ground plane may influence the firing of dorsal grid cells with narrower spacing between firing fields. These sensory influences could contribute to the potential functional role of grid cells in guiding goal-directed navigation.

Corresponding author M. E. Hasselmo: Centre for Systems Neuroscience, Center for Memory and Brain, Department of Psychological and Brain Sciences and Graduate Program for Neuroscience, Boston University, 2 Cummington Mall, Boston, MA 02215, USA.   Email: hasselmo@bu.edu

Abstract figure legend This figure shows the activity pattern of a single grid cell recorded from the medial entorhinal cortex of a rat as it forages in a circular environment with a boundary wall. The mean firing rate of the cell increases (red) when the rat visits an array of locations within the environment corresponding to vertices of tightly packed equilateral triangles. The location-specific firing could partly depend on computation of spatial location based on the angle of visual stimuli the rat observes in its visual field, or based on optic flow of visual stimuli on the ground plane.

Abbreviations   GABA, gamma-aminobutyric acid; mEC, medial entorhinal cortex.

Modelling the sensory influences on spatial firing of entorhinal neurons

The behaviour of many different mammalian species requires the accurate coding of spatial location in the environment, ranging from the foraging behaviour of rodents to the social interactions of humans. Research in rodents and humans indicates that the neural mechanisms for coding of space appear to include neuronal spiking activity of place cells in the hippocampus (O'Keefe & Dostrovsky, 1971; O'Keefe, 1976; O'Keefe & Nadel, 1978) and grid cells in the medial entorhinal cortex (mEC) (Fyhn *et al.* 2004; Hafting *et al.* 2005; Moser & Moser, 2008; Jacobs *et al.* 2013). Place cells fire when an animal visits specific individual spatial locations in an environment, while grid cells in the mEC fire during visits to a regular array of locations that fall on the vertices of a hexagonal grid across an environment. These neuronal populations are clearly not the only mechanism of spatial localization, as humans with medial temporal lobe damage, such as the patient known as H.M., can find their way around familiar environments (Scoville & Milner, 1957; Milner *et al.* 1968). Similarly, rats with hippocampal lesions are not impaired in the use of reference memory to avoid unrewarded arms in an eight-arm radial maze (Olton *et al.* 1979, 1986) and can still navigate to a specific location, though their learning is much slower (Morris *et al.* 1982). However, these structures appear important for rapidly encoding

new spatial locations in unfamiliar, novel environments (Olton *et al.* 1979, 1986; Morris *et al.* 1982), and hence their accurate updating on the basis of sensory features appears to be essential to memory-guided behaviour in new environments.

This review will focus on models of the role of sensory input during self-motion in determining the firing properties of grid cells. This will draw on extensive experimental data showing the response of neurons in entorhinal cortex to manipulations of sensory features in the environment. On a broad scale, location can be computed in either relative or absolute coordinates. Absolute coordinates would index Cartesian coordinates for location relative to the same origin (0, 0) on multiple visits to an environment. In contrast, relative coordinates would update location based on some arbitrary starting coordinate. For example, the relative coordinate shift of (2, 3) on different visits would be the same for the transition from a first absolute starting location (1, 2) to (3, 5) and for the transition from a second absolute starting location (5, 11) to (7, 14). Absolute location can be coded by reference to the static distance and angle of sensory features (such as visual or auditory stimuli). Relative location can be computed based on sensory features from self-motion (including both proprioceptive feedback and motor efference copy concerning generated movements, as well as moving sensory features such as optic flow or whisker input). The terms absolute and relative location

will be discussed repeatedly in this review, and we will also refer to static sensory features, moving sensory features, proprioceptive feedback and efference copy of self-motion.

Relative location from proprioceptive and efference copy of self-motion signals

Many early models of grid cells focused on path integration from the running velocity of the animal (the speed and direction of movement) based on the integration of the motor output. These early models did not directly address the computation of speed and movement direction. Instead, these models usually assumed that these properties can be computed from proprioceptive feedback or efference copy of self-motion signals from motor command centres, but as reviewed here they could also be computed from moving sensory features.

Input about running velocity was used to drive the majority of models of grid cells using attractor dynamics (Fuhs & Touretzky, 2006; McNaughton *et al.* 2006; Guanella *et al.* 2007; Burak & Fiete, 2009; Giocomo *et al.* 2011; Pastoll *et al.* 2013). These models generate the grid cell firing pattern across a wide population of neurons, and then shift the current location coded by the population based on velocity input provided by structured connectivity of conjunctive grid-by-head-direction cells (McNaughton *et al.* 2006; Burak & Fiete, 2009). In these models, the population pattern of grid cell firing is driven by circularly symmetric excitatory or inhibitory recurrent synapses. This results in a major strength of these models in accounting for experimental data on shared orientation and spacing of firing fields (Sargolini *et al.* 2006; Stensola *et al.* 2012), and the quantal nature of grid cell spacing in different modules (Barry *et al.* 2007; Stensola *et al.* 2012). These models are also supported by recent data supporting circular symmetry of synaptic interactions between grid cells (Heys *et al.* 2014). The use of velocity input in these attractor models means that most existing simulations of these models compute relative location. However, these models could be modified to compute absolute location based on direct associations between specific patterns of sensory feature input indicating position and specific subpopulations of neurons within the population as done in a recent model (Bush & Burgess, 2014).

Velocity input was also used as input in a class of grid cell models using oscillatory interference (Burgess *et al.* 2005, 2007; Blair *et al.* 2008; Burgess, 2008; Hasselmo, 2008; Welday *et al.* 2011). In these models, individual grid cells are driven by input from multiple velocity-controlled oscillators that change frequency based on current speed and the current movement direction relative to the preferred direction angle of individual oscillators. These oscillatory interference models effectively simulate the theta rhythmic firing of grid cells (Hafting *et al.* 2008;

Jeewajee *et al.* 2008; Brandon *et al.* 2011; Koenig *et al.* 2011; Stensola *et al.* 2012), and the changes in rhythmic firing frequency based on running speed and the spacing between firing fields (Jeewajee *et al.* 2008; Stensola *et al.* 2012).

Because these oscillatory interference models arose from models of theta phase precession in the hippocampus (O'Keefe & Recce, 1993; Skaggs *et al.* 1996; Lengyel *et al.* 2003), these models effectively account for the theta phase precession of grid cells (Hafting *et al.* 2008; Climer *et al.* 2013; Eggink *et al.* 2014) and the prominent theta in the local field potential of entorhinal cortex (Mitchell & Ranck, 1980; Mitchell *et al.* 1982; Alonso & Garcia-Austt, 1987; Jeffery *et al.* 1995). Models related to oscillatory interference (Hasselmo & Shay, 2014) can also address theta cycle skipping in the medial septum (King *et al.* 1998; Varga *et al.* 2008) and mEC (Jeffery *et al.* 1995; Deshmukh *et al.* 2010; Brandon *et al.* 2013) and firing of different populations on opposite phases of theta (Mizuseki *et al.* 2009; Newman & Hasselmo, 2014). Attractor models have only simulated phase precession during one-dimensional movement (Navratilova *et al.* 2012).

Oscillatory interference can be successfully merged with attractor dynamics (Bush & Burgess, 2014). Such a merger accounts for data showing depolarizations in grid cell firing fields without changes in envelopes of theta oscillations (Domnisoru *et al.* 2013; Schmidt-Hieber & Hausser, 2013). Oscillatory interference models can compute absolute location either through sensory input to drive a subpopulation of cells (Bush & Burgess, 2014), or by updating oscillation phase using visual features (Burgess, 2008). Variants of these models generate the periodicity in the firing of grid cells using ring oscillators (Blair *et al.* 2008, 2014; Welday *et al.* 2011) or using wave inputs (Hasselmo & Brandon, 2012; Hasselmo, 2014; Hasselmo & Shay, 2014).

An additional class of models uses self-organization of feedforward signals from place cells (Kropff & Treves, 2008; Mhatre *et al.* 2010; Si *et al.* 2012) providing coding of absolute location in grid cells that depends upon place cell firing. As an alternative, some attractor models use global input to entorhinal cortex from place cells in hippocampus to account for the loss of grid cell firing during inactivation of the hippocampus (Bonnevie *et al.* 2013).

The focus of many models on path integration with a self-motion signal was partly due to data showing that grid cells continue to show regular firing fields in darkness (Hafting *et al.* 2005), suggesting that they do not require visual sensory input. However, studies have not analysed the dependence of grid cells on other sensory input such as somatosensory input from whisking or auditory localization input. The question remains whether path integration based on proprioceptive feedback and efference copy of motor signals for

self-motion can generate grid cells in isolation from other sensory influences. Studies in absolute darkness should be combined with the use of sound attenuation chambers and clipping of whiskers to remove these components of sensory input so that the animal must solely rely on proprioceptive, efference copy and vestibular self-motion signals.

Head direction dominates over movement direction

As noted above, the self-motion signal could come from either internal signals (proprioceptive feedback or efference copy) or from sensory input. The use of a proprioceptive self-motion signal must assume that the grid cells in mEC have access to proprioceptive feedback or efference copy coding both translational speed and movement direction to create a velocity signal. As noted above, the use of velocity input is present in most published attractor dynamic models (Fuhs & Touretzky, 2006; McNaughton *et al.* 2006; Guanella *et al.* 2007; Burak & Fiete, 2009; Bonnevie *et al.* 2013; Couey *et al.* 2013; Pastoll *et al.* 2013) as well as oscillatory interference models (Burgess *et al.* 2007; Blair *et al.* 2008; Burgess, 2008; Hasselmo, 2008; Zilli & Hasselmo, 2010). Thus, these models use input of both speed and movement direction.

The requirement of a speed signal is supported by data showing examples of linear and saturating exponential relationships of firing rate to running speed in recordings from hippocampus and mEC (O'Keefe *et al.* 1998; Wills *et al.* 2012; Kemere *et al.* 2013; Kropff *et al.* 2015; Hinman JR, Brandon MP, Chapman GW, Climer JR & Hasselmo ME, submitted). The important role of speed in these models is further supported by data on changes in the frequency of spiking in the medial septum (King *et al.* 1998) or theta frequency field potentials in hippocampus during changes in running speed (Hinman *et al.* 2011). This indicates a potentially important role of the input from the medial septum to the hippocampus. It is possible that the impairments of spatial memory caused by inactivation of the medial septum (Chrobak *et al.* 1989) are due to loss of a speed signal input from medial septum. This is further supported by data showing the loss of spatial periodicity of grid cells when network theta rhythm oscillations are reduced by inactivation of the medial septum (Brandon *et al.* 2011; Koenig *et al.* 2011). It is not yet clear which cell population underlies this effect, as the medial septum inactivation in those previous studies (Brandon *et al.* 2011; Koenig *et al.* 2011) would involve simultaneous inactivation of cholinergic, GABAergic and glutamatergic neurons. Recent data show that phasic optogenetic activation at theta frequency of glutamatergic neurons in the medial septum triggers running by mice at speeds regulated by the frequency of optogenetic stimulation (Fuhrmann *et al.* 2015). These

data on coding of translational speed by the medial septum support models using translational speed as a component of a velocity signal for grid cell generation.

However, the requirement of models for movement direction is more problematic, despite the fact that many papers cite head direction responses of mEC as the evidence for a movement direction signal. Head direction cells are one of the most dramatic neural responses to spatial dimensions found in the brain. Head direction cells were initially discovered in the dorsal presubiculum (Ranck, 1984; Taube *et al.* 1990*a,b*) and subsequently described in the anterior thalamus (Taube, 1995) and mEC (Sargolini *et al.* 2006). Head direction cells clearly depend upon input from the vestibular system coding angular velocity (the turning speed of the head), but also show dependence upon visual cues (Taube *et al.* 1996; Taube & Bassett, 2003). Many attractor models use grid-by-head-direction cells to shift the grid cell population activity during movement (McNaughton *et al.* 2006; Burak & Fiete, 2009; Couey *et al.* 2013), and equate head direction with movement direction.

However, an analysis of behavioural data shows that the head direction signal does not match movement direction (Fig. 1*A*). Because of this, when behavioural data on head direction is used as input to attractor models or oscillatory interference models in place of a behavioural movement direction signal, the models do not generate accurate grid cell firing (Raudies *et al.* 2015) as shown in Fig. 1*E* and *F*. This occurs because the integration of velocity in those models is distorted by the use of head direction instead of movement direction. Further analysis of experimental data on the firing properties of a large population of medial entorhinal neurons during periods when head direction does not match movement direction shows little evidence for neurons coding a movement direction signal (Raudies *et al.* 2015). In the data, numerous neurons clearly code head direction alone, but only a few neurons code both head direction and movement direction and no neurons respond on the basis of movement direction alone (Fig. 1*C* and *D*). One possibility is that the movement direction signal is present in other regions and may drive the mechanisms of the firing of grid cells in other networks such as the pre- or parasubiculum (Boccara *et al.* 2010) without being evident in medial entorhinal cortex. As an alternative hypothesis, this stronger coding of head direction and relative lack of a movement direction signal suggests that a self-motion signal might rely less on internal signals of movement direction and instead may depend on a representation of the head direction for coding sensory input. The coding of the head direction angle would allow the computation of the absolute angle of visual, auditory and somatosensory input because these sensory inputs are initially detected in terms of their angle relative to coordinates centred on current head direction.
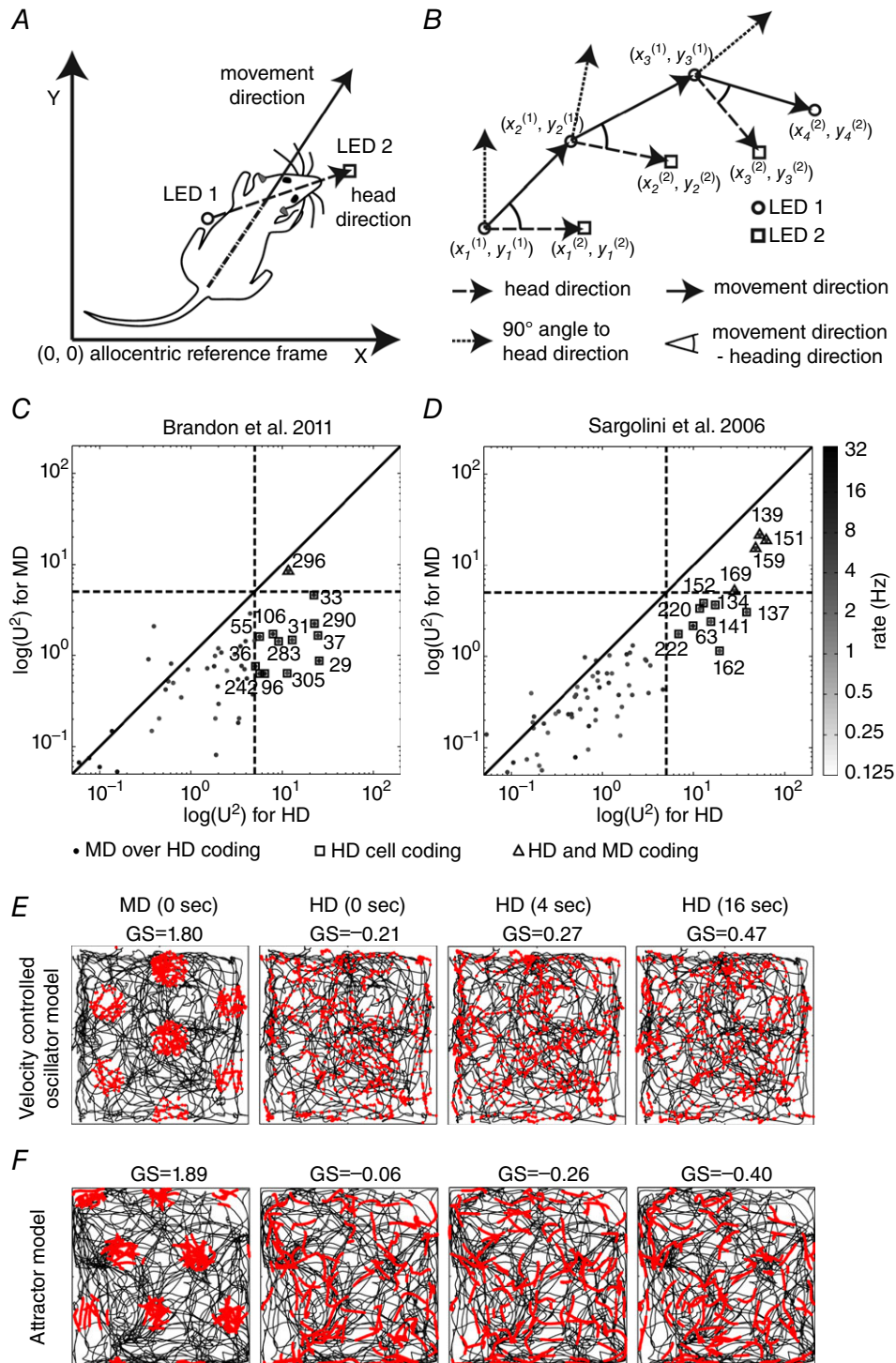
Figure 1. Analysis of single cell recording data from entorhinal cortex for head direction (HD) and movement direction (MD) along with a model simulation of grid cells using HD or MD as input

A, we infer the head direction through the orientation given by the two LEDs, 1 and 2, and the movement direction taking the temporal advancement of the mid-point between LED 1 and 2. *B*, a sketched sequence for the temporal succession of the positional sample points of LED 1 and 2 to illustrate the definition of HD, MD and the angular difference between HD and MD. *C*, the Watson U^2 for the population of 305 cells from the Hasselmo laboratory. *D*, the Watson U^2 for the population of 453 cells from the Moser laboratory. Plotted points of the Watson U^2 for MD tuning versus Watson U^2 for HD tuning are from the same cell. Axes are log-scaled as are the grey values that represent the firing rate of each cell in hertz. Cells whose Watson U^2 pair is below the diagonal primarily

Optic flow can drive grid cells and boundary vector cells

The dominant coding of head direction by cells in the mEC supports the importance of sensory input in coding of grid cells. The influence of sensory input on grid cells has not been explicitly discussed as extensively as path integration based on proprioceptive self-motion. However, a modelling study showed how optic flow of visual features could be used to compute a velocity signal to drive grid cell models using attractor dynamics or oscillatory interference (Raudies *et al.* 2012). This model used template matching of optic flow to estimate velocity, and then used the estimated velocity to compute the relative location in a grid cell model (Fig. 2*D*). Note that this model did not compute absolute location.

As shown in Fig. 2, optic flow can also be used as sensory input to model the generation of boundary cells (Raudies & Hasselmo, 2012). Boundary cells in mEC and subiculum show robust spiking responses dependent on the distance and angle of environmental boundaries (Burgess *et al.* 2000; Barry *et al.* 2006; Savelli *et al.* 2008; Solstad *et al.* 2008; Lever *et al.* 2009). For example, they might respond when an environmental boundary is to the north of an animal at a specific distance. In an important theoretical model, these boundary cells were predicted (Burgess *et al.* 2000; Hartley *et al.* 2000) based on the response of place cells to manipulations of environmental barriers (O'Keefe & Burgess, 1996). For example, if the east–west distance between boundaries of an environment is expanded, then the size of a place field may expand in the east–west dimension, or the cell may split into two firing fields. These properties of place cells were modelled using boundary vector cells with properties that were extensively analysed in computational work (Burgess *et al.* 2000; Hartley *et al.* 2000).

The explicit predictions of these models were then supported by the later experimental discovery of these cells (Barry *et al.* 2006; Savelli *et al.* 2008; Solstad *et al.* 2008; Lever *et al.* 2009). Boundary cells allow for analysing the absolute distance and angle of environmental boundaries from the current position of an animal. As shown in Fig. 2*A–C*, optic flow was used to model the firing of boundary cells (Fig. 2*E*) through detection of a discontinuity in the optic flow at the border between a wall and the ground plane of the environment (Raudies & Hasselmo, 2012). Note that though this model uses optic flow, because it detects the distance and angle of a boundary, it is computing absolute location in the environment and could be used to drive the absolute location of grid cell firing or place cell firing, as proposed in the initial models of boundary vector cells (Burgess *et al.* 2000; Hartley *et al.* 2000).

Absolute location from static sensory features

Experimental data on grid cells indicate the influence of sensory input on their firing properties. For example, grid cells fire in the same spatial location in a specific experimental environment even after the animal has been removed from the room and returned to the room (Hafting *et al.* 2005; Fyhn *et al.* 2007), indicating that grid cells not only track location relative to the initial position, but are able to reinstate the appropriate location activity based on sensory cues when reintroduced to a previously visited environment. The sensory cues regulating the location of grid cell firing include visual cues in the environment. Rotation of the position of a white cue card on the wall of an environment between recording sessions will cause grid cells to rotate according to the rotation of the cue card (Hafting *et al.* 2005). In addition, shifting the position of the walls of the environment between sessions causes compression or expansion of the spacing and size of grid cell firing fields temporarily (Barry *et al.* 2007). After adaptation to the alteration in the environment the grid cell firing fields return to their previous hexagonal firing pattern. Further experimental studies showed that this shift in the position of the walls affects grid cells with large spacing between firing fields more so than cells with small spacing (Stensola *et al.* 2012).

These effects of boundary movement could partly be due to close somatosensory interactions with the boundaries, as the firing accuracy of grid cells depends upon the recency of interaction with boundaries in the environment (Hardcastle *et al.* 2015). A recent model has shown that the influence of boundary cells could alter the positioning of grid cell firing fields based on different shapes of environments (Krupic *et al.* 2014), correctly predicting that an environment with trapezoid walls would have distorted firing field location as supported by recent data from grid cells (Krupic *et al.* 2015).

encode HD, whereas those above the diagonal primarily encode MD. The distribution of cells is predominantly biased toward statistical encoding of HD rather than MD. Numbers denote cell indices. Dashed lines mark the threshold of 5 for the U^2s that we used to categorize HD and MD cells. Plotted squares around points indicate HD coding and plotted triangles around points indicate combined HD and MD coding. *E*, simulations of the velocity controlled oscillator (VCO) model (top row) and attractor model (bottom row) with MD or HD as directional input. The speed input was that of the measured trajectory. Different panels show the simulated cell firing for the HD or MD while integrating over a 0, 4 or 16 s time window. Whenever HD is provided as input no grid cell firing appears (last three columns in *E* and *F*). In contrast, the direct input of MD (0 s time window) produces grid cell firing (first column in *E* and *F*). Adapted from Raudies *et al.* (2015).

As shown in Fig. 3, recent modelling work has shown that differential sensitivity to boundary movement could arise from differences in the nature of simulated location computation by different grid cell modules (Raudies & Hasselmo, 2015). The term module refers to populations of grid cells that have been shown to share firing field properties such as orientation and spacing between fields (Barry *et al.* 2007; Stensola *et al.* 2012). Modelling shows that modules sensitive to static visual features on the walls of the environment (Fig. 3*A–F*) would be particularly sensitive to the shift of the visual features with wall movement (Raudies & Hasselmo, 2015), as shown in

experimental data (Barry *et al.* 2007; Stensola *et al.* 2012). In contrast, modelling shows that modules responding to visual features on the ground plane near the rat would be less sensitive to wall movement (Fig. 3*G–I*), particularly if the firing location is driven by integration of a moving feature signal from the ground plane near the rat (Raudies & Hasselmo, 2015). This could explain the lack of compression of firing fields for grid cells with smaller spacing (Stensola *et al.* 2012). Cells with smaller spacing between firing fields tend to occur in more dorsal anatomical locations that might be more sensitive to the ventral visual field.
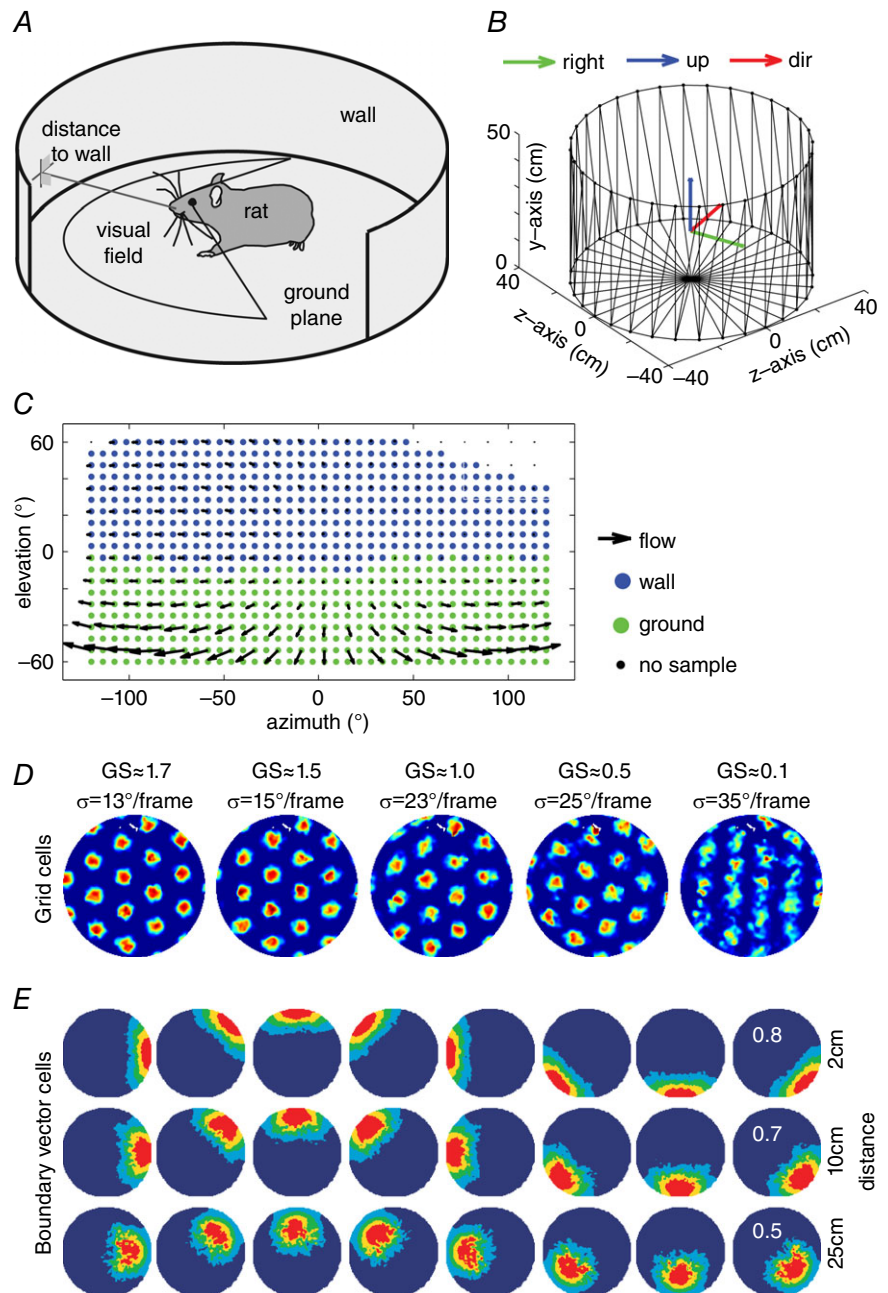

Figure 2. Modelled firing patterns of simulated grid cells and boundary vector cells using optic flow as input
A, a rat in a circular box with a depiction of its distance to the wall. *B*, simulated box environment for boundary vector cells. The coordinate system (red, blue and green arrows) indicates the initial position and orientation of the simulated visual field of the rat. *C*, an optic flow field for a spherical camera with its segmentation into ground plane (green dots) and wall (blue dots). This optic flow field is used to estimate the linear and rotational velocity of the rat as well as the distance of the wall in ego-centric space and the orientation of the wall in allo-centric space. Adapted from Raudies & Hasselmo (2012). *D*, simulated grid cell firing using the oscillatory interference model while superimposing independent, additive Gaussian noise onto the optic flow components with a standard deviation σ of 13, 15, 23, 25 and 35 deg frame^{-1}. The simulated grid cell firing vanishes above a standard deviation of $\sigma \approx 23$ deg frame^{-1}. The simulation uses the trajectory 'Hafting_Fig2C_Trial1' from Hafting *et al.* (2005). The box has a diameter of 100 cm with a 15 cm annulus added to provide visual features beyond the limits of locomotion. Adapted from (Raudies *et al.* 2012). *E*, the rate map of our model for boundary vector cells when estimating distance and direction of walls from optic flow. The box has a diameter of 79 cm and the height of the wall is 50 cm.

The selective effect on individual modules suggests differences in the anatomical pathways of visual feature processing reaching different portions of mEC. In the rodent visual system, some regions (e.g. area AM) respond more strongly to grating stimuli with high temporal frequency (movement) and low spatial frequency, other regions (e.g. area PM) respond more to low temporal frequency (more static stimuli) with higher spatial frequency, and yet other regions respond to a mixture (area LM) (Andermann *et al.* 2011; Wang *et al.* 2011, 2012; Glickfeld *et al.* 2014). These responses might indicate differential processing in the rodent similar to the distinction between the 'where' and 'what' pathways described extensively for the dorsal and ventral streams of the primate cortex (Ungerleider & Mishkin, 1982). Note that the primate extrastriate visual cortex contains regions that explicitly respond to the self-motion indicated by optic flow (Rodman & Albright, 1987; Graziano *et al.* 1994; Duffy & Wurtz, 1995). These pathways might correspond to differential visual processing inputs, with optic flow signals entering the dorsal mEC *versus* the landmark signals entering the ventral mEC. Alternately, these might reflect the differential influence of input from different portions of the visual field, with dorsal mEC responding
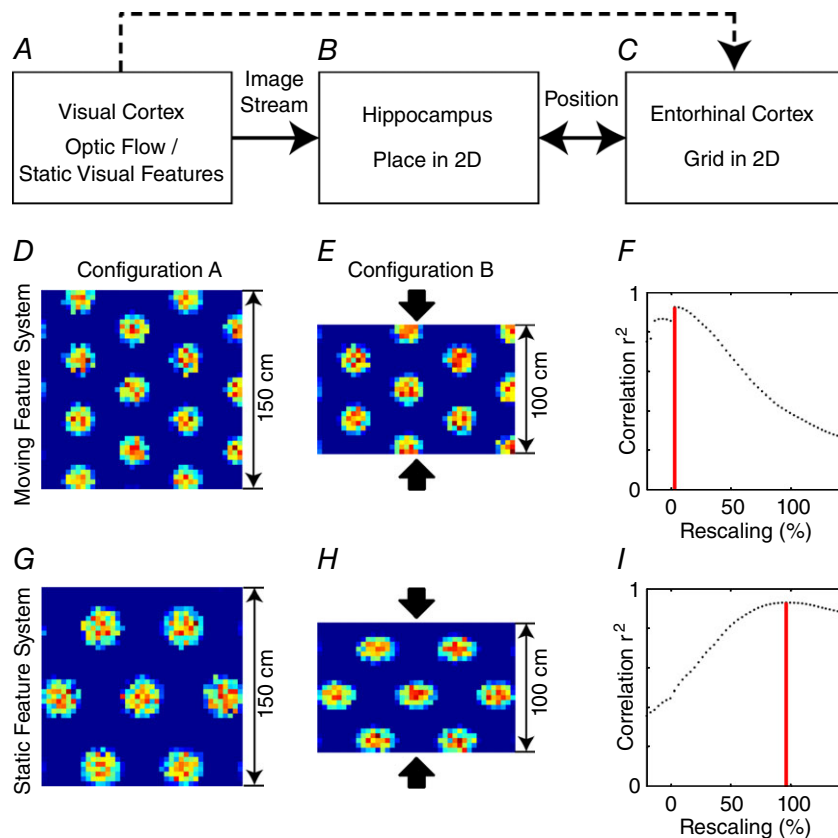

Figure 3. A model of compression effects that occur in grid cells from modules that map to the ventral visual field but not in grid cells from modules that map to the dorsal visual field
A, the visual cortex processes optic flow and visual features. Optic flow is strongly present on the ground plane in the ventral visual field whereas distal visual features in the dorsal visual field make good landmarks. *B*, via multiple processing stages, optic flow and visual features influence hippocampal activity, giving rise to a place-specific firing in a 2D environment. *C*, in the entorhinal cortex this 2D place information is translated into the firing of grid cells. Our model has two modules, one that estimates location from optic flow on the ground plane and one that estimates location from static visual features on the walls through triangulation. The anatomical projections from visual cortex to entorhinal cortex are not currently used in our model as shown by the dashed line. *D, E, G* and *H*, in configuration A the box is square (*D* and *G*) and in configuration B the box is rectangular (*E* and *H*) after pushing two opponent walls closer together (when the rat is outside of the box). For the moving feature system responding to the ground plane in the ventral visual field this compression of walls left the firing pattern of a simulated dorsal entorhinal cell unchanged (see *D vs. E*), while for the static feature system responding to distal features in the dorsal visual field this led to a compression of the firing pattern of a simulated ventral entorhinal cell (see *G vs. H*). *F*, for the firing pattern of the simulated dorsal entorhinal cell correlation values for different compressions of B relative to A, there is a peak correlation at ∼3.1% compression. *I*, for the firing pattern of the simulated ventral entorhinal cell, correlation values peak at ∼95.5% (or about 50 cm) compression of B relative to A.

to features on the ground plane whereas ventral mEC responds to features on distal walls.

Computing location from full visual images

The model described above simulated differential effects on grid cell firing field spacing used the relative angle of pre-defined visual features, but there are also models that have addressed the use of more detailed visual images in driving spatial responses of grid cells. For example, a paper used a ray-tracing algorithm to create images of a rat environment to drive the firing responses of oriented Gabor filters that could drive an attractor model of grid cells (Sheynikhovich *et al.* 2009). This explicit simulation of visual input is rare, but other models assume that sensory input can provide a position signal to periodically correct the firing location of grid cells (Burgess *et al.* 2007; Pastoll *et al.* 2013; Bush & Burgess, 2014) or use slow feature extraction to drive grid cells (Franzius *et al.* 2007). Recent work in our laboratory addresses the mechanism for generating a position signal from visual input based on previous robotics work by Michael Milford (Milford, 2008; Milford & Wyeth, 2008, 2010; Milford *et al.* 2010; Chen *et al.* 2014). The effectiveness of the visual input depends upon an appropriate Gaussian tuning width for detection of visual features that allows generalization between adjacent locations without over-generalizing. In a recent model shown in Fig. 4 (F. Raudies and M. E. Hasselmo, unpublished), this position signal was used as input to different models of grid cells, and the sensitivity of the models to external position noise was evaluated. A similar analysis of sensitivity to external position noise was evaluated recently (Towse *et al.* 2014).

Note that the external position noise used in the model in Fig. 4 and the Towse paper differs from most previous noise evaluations in grid cell models, in that external noise rather than internal noise and position noise rather than velocity noise were used. Internal noise causes problems for oscillatory interference models (Burgess *et al.* 2007; Zilli *et al.* 2009), but can be overcome by attractor dynamics (Burak & Fiete, 2009; Bush & Burgess, 2014). In contrast, both attractor dynamic models and oscillatory interference models have difficulty in overcoming the external noise in a velocity signal because attractor dynamics overcome the noise of internal dynamics but not the noise on an input signal. The problem of external noise is somewhat less severe when the noise affects a position signal based on sensory input rather than a velocity signal from self-motion because the integration of a velocity signal by the model results in integration of the noise over time, whereas noise on a position signal is not integrated. In the simulations shown here, visual input is used to create a position signal that is provided as input to models of grid cells. Noise is then added to this position signal to determine its impact on different grid cell models.

In the model shown in Fig. 4 (Raudies and Hasselmo, unpublished model), the generation of synthesized rat trajectories provides the position signals for our renderer that generates images for each position. Such memorized images are then used to retrieve position through normalized cross-correlation, which in turn is fed into our proposed wave model. This wave model resembles previous oscillatory interference models (Burgess *et al.* 2007) and ring oscillator models (Blair *et al.* 2008). The wave model generates grid cell firing across a population with waves representing medial septal input that are summed to compute grid cell firing (Hasselmo & Brandon, 2012; Hasselmo & Shay, 2014). Feedback from the grid cells to the wave input results in self-organization that selectively strengthens input from sets of waves with specific head direction orientations at 60 degree intervals. In a separate analysis performed for comparison with the wave model, the position signal is temporally differentiated to define a velocity signal that is then fed into an attractor model or oscillatory interference model. Our results present properties of the wave model and compare our wave model using position input from visual stimuli to the attractor model or oscillatory interference model using self-motion velocity input. The use of position input based on visual stimuli can tolerate more noise than the use of self-motion velocity input even when equating the signal-to-noise ratio of the noise in the velocity with the noise in the position signal.

Models of goal-directed navigation using grid cells and place cells

Behavioural data indicate that humans and animals do not need the hippocampus and entorhinal cortex to navigate in a familiar environment. The mechanisms of navigation in highly familiar environments appears to depend upon neocortical regions such as the parietal cortex (Byrne *et al.* 2007). However, entorhinal cortex and hippocampus may be essential for the formation of spatial representations and goal-directed navigation within novel environments (Milford *et al.* 2010; Erdem *et al.* 2015), to allow behaviours such as forward planning of trajectories to goal locations (Erdem & Hasselmo, 2012, 2014; Erdem *et al.* 2015). In these models, the current head direction can be used to trigger forward replay of a trajectory through the environment, to allow for the selection of a trajectory that will overlap with a desired goal location. In this framework, the coding of visual stimuli (Milford *et al.* 2010) allows for the correction of position errors that could distort goal-directed navigation (Erdem *et al.* 2015). A similar framework can be used to model episodic memory (Hasselmo, 2009, 2012), in which specific locations and head direction along a spatiotemporal trajectory can be
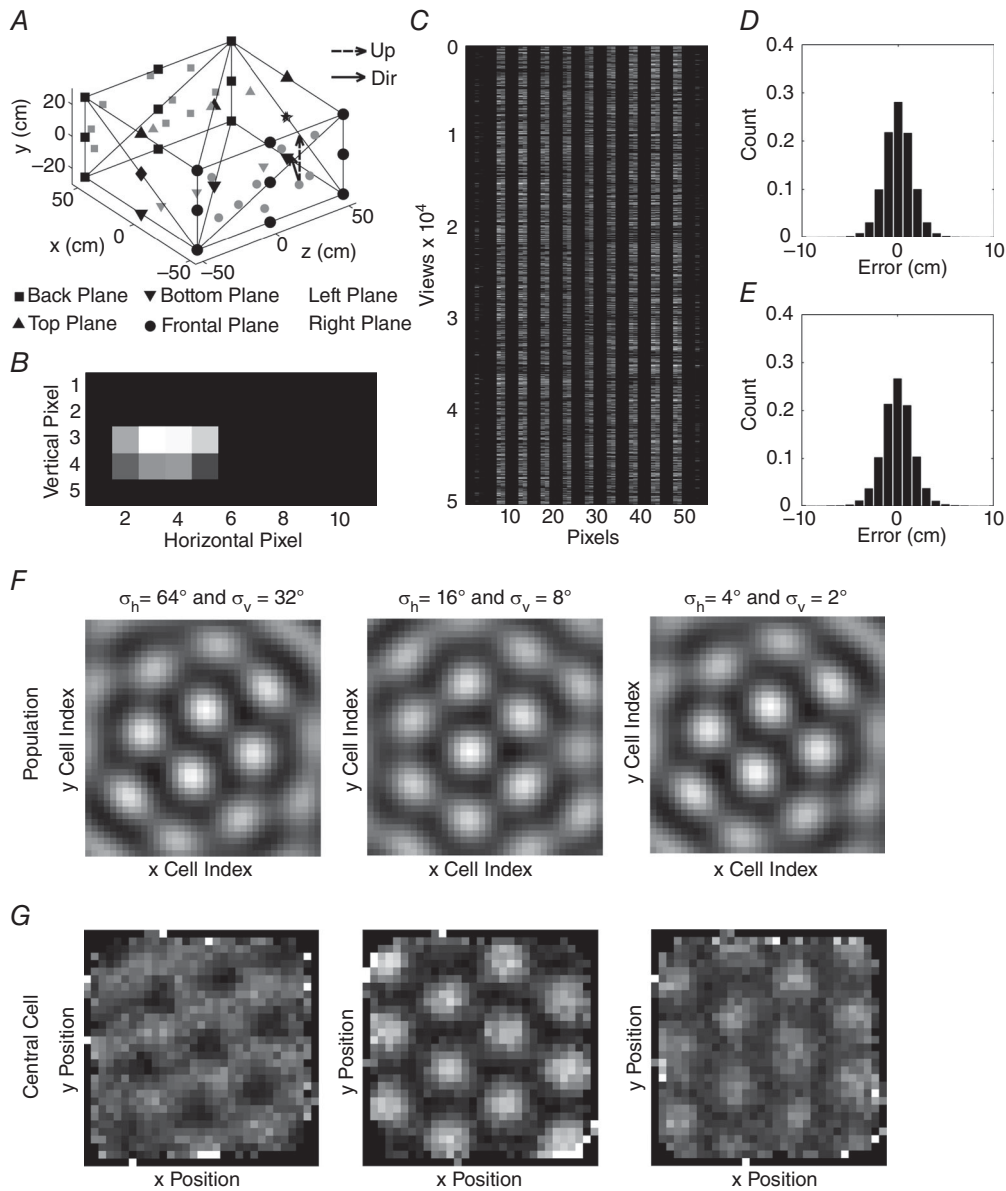
Figure 4. The simulation of grid cells using a wave model that is driven by the position signal that in turn is retrieved from visual views

A, enclosure used in the simulation with ground (downward triangle), side walls (square, circle, diamond and star symbols), and ceiling (upward triangle) – in the actual simulation the lines were not present. Black symbols show the positions of features before random displacement on their associated surface (i.e. ground, walls or ceiling). Scattered features are drawn as grey symbols. All features were identical for the actual generation of an image. *B*, exemplar image for the camera position indicated in *A* by the direction (Dir) vector and upward vector (Up). Bright regions indicate the overlay of 2D Gaussian blobs generated by features. *C*, stored images for 50,000 sample points and 11 pixel × 5 pixel or 55 total pixel values. Grey values for pixels in the image are flattened along the vertical dimension. *D*, position errors for retrieval in the horizontal direction are fitted by a normal distribution with zero mean and a standard deviation of 2.79 cm. *E*, position errors in the vertical direction are fitted by a normal distribution with zero mean and a standard deviation of 3.10 cm. *F*, population responses and firing pattern of the central cell for images generated by 2D Gaussians with $\sigma_h = 64°$ and $\sigma_v = 32°$ (fist column), $\sigma_h = 16°$ and $\sigma_v = 8°$ (second column), and $\sigma_h = 4°$ and $\sigma_v = 2°$ (third column). The population response at a single time step in *F* shows that the wave model always generates a hexagonal grid pattern at individual time steps. Bright encodes a high activation and dark a low activation of cells. *G*, firing patterns of the central cell in the population were recorded over 50,000 sample steps. This shows how accurately the population activity is shifted over time by the estimate of position based on visual input, in order to allow a single cell to fire like a grid cell during the full trajectory. Bright indicates a high firing rate and dark indicates a low firing rate. The GSs are −0.37, 1.91 and 0.93 for the first, second and third column, respectively, indicating best performance with the intermediate Gaussian widths that allow best generalization of visual images over nearby positions.

associated with sensory input features via modifications of synaptic connections. During replay or recollection, a retrieval cue activating a specific segment of the trajectory can trigger retrieval of other segments and the associated sensory input features. Models of this type could address the physiological data on replay of previously encoded sequences of place cells observed in behaving rats (Johnson & Redish, 2007; Mehta, 2007; Davidson *et al.* 2009; Jadhav *et al.* 2012).

References

Alonso A & Garcia-Austt E (1987). Neuronal sources of theta rhythm in the entorhinal cortex of the rat. I. Laminar distribution of theta field potentials. *Exp Brain Res* **67**, 493–501.

Andermann ML, Kerlin AM, Roumis DK, Glickfeld LL & Reid RC (2011). Functional specialization of mouse higher visual cortical areas. *Neuron* **72**, 1025–1039.

Barry C, Hayman R, Burgess N & Jeffery KJ (2007). Experience-dependent rescaling of entorhinal grids. *Nat Neurosci* **10**, 682–684.

Barry C, Lever C, Hayman R, Hartley T, Burton S, O'Keefe J, Jeffery K & Burgess N (2006). The boundary vector cell model of place cell firing and spatial memory. *Rev Neurosci* **17**, 71–97.

Blair HT, Gupta K & Zhang K (2008). Conversion of a phase- to a rate-coded position signal by a three-stage model of theta cells, grid cells, and place cells. *Hippocampus* **18**, 1239–1255.

Blair HT, Wu A & Cong J (2014). Oscillatory neurocomputing with ring attractors: a network architecture for mapping locations in space onto patterns of neural synchrony. *Philos Trans R Soc Lond B Biol Sci* **369**, 20120526.

Boccara CN, Sargolini F, Thoresen VH, Solstad T, Witter MP, Moser EI & Moser MB (2010). Grid cells in pre- and parasubiculum. *Nat Neurosci* **13**, 987–994.

Bonnevie T, Dunn B, Fyhn M, Hafting T, Derdikman D, Kubie JL, Roudi Y, Moser EI & Moser MB (2013). Grid cells require excitatory drive from the hippocampus. *Nat Neurosci* **16**, 309–317.

Brandon MP, Bogaard AR, Libby CP, Connerney MA, Gupta K & Hasselmo ME (2011). Reduction of theta rhythm dissociates grid cell spatial periodicity from directional tuning. *Science* **332**, 595–599.

Brandon MP, Bogaard AR, Schultheiss NW & Hasselmo ME (2013). Segregation of cortical head direction cell assemblies on alternating theta cycles. *Nat Neurosci* **16**, 739–748.

Burak Y & Fiete IR (2009). Accurate path integration in continuous attractor network models of grid cells. *PLoS Comput Biol* **5**, e1000291.

Burgess N (2008). Grid cells and theta as oscillatory interference: theory and predictions. *Hippocampus* **18**, 1157–1174.

Burgess N, Barry C, Jeffery KJ & O'Keefe J (2005). A grid and place cell model of path integration utilizing phase precession versus theta. Poster presented at the Computational Cognitive Neuroscience Conference, Washington DC, 10–11 November 2005. http://cdn.f1000.com/posters/docs/225.

Burgess N, Barry C & O'Keefe J (2007). An oscillatory interference model of grid cell firing. *Hippocampus* **17**, 801–812.

Burgess N, Jackson A, Hartley T & O'Keefe J (2000). Predictions derived from modelling the hippocampal role in navigation. *Biol Cybern* **83**, 301–312.

Bush D & Burgess N (2014). A hybrid oscillatory interference/continuous attractor network model of grid cell firing. *J Neurosci* **34**, 5065–5079.

Byrne P, Becker S & Burgess N (2007). Remembering the past and imagining the future: a neural model of spatial memory and imagery. *Psychol Rev* **114**, 340–375.

Chen Z, Jacobsen A, Erdem UM, Hasselmo ME & Milford MJ (2014). Multi-scale bio-inspired place recognition. *2014 IEEE International Conference on Robotics and Automation (ICRA)*, 1895–1901; doi: 10.1109/ICRA.2014.6907109.

Chrobak JJ, Stackman RW & Walsh TJ (1989). Intraseptal administration of muscimol produces dose-dependent memory impairments in the rat. *Behav Neural Biol* **52**, 357–369.

Climer JR, Newman EL & Hasselmo ME (2013). Phase coding by grid cells in unconstrained environments: two-dimensional phase precession. *Eur J Neurosci* **38**, 2526–2541.

Couey JJ, Witoelar A, Zhang SJ, Zheng K, Ye J, Dunn B, Czajkowski R, Moser MB, Moser EI, Roudi Y & Witter MP (2013). Recurrent inhibitory circuitry as a mechanism for grid formation. *Nat Neurosci* **16**, 318–324.

Davidson TJ, Kloosterman F & Wilson MA (2009). Hippocampal replay of extended experience. *Neuron* **63**, 497–507.

Deshmukh SS, Yoganarasimha D, Voicu H & Knierim JJ (2010). Theta modulation in the medial and the lateral entorhinal cortices. *J Neurophysiol* **104**, 994–1006.

Domnisoru C, Kinkhabwala AA & Tank DW (2013). Membrane potential dynamics of grid cells. *Nature* **495**, 199–204.

Duffy CJ & Wurtz RH (1995). Response of monkey MST neurons to optic flow stimuli with shifted centres of motion. *J Neurosci* **15**, 5192–5208.

Eggink H, Mertens P, Storm E & Giocomo LM (2014). Hyperpolarization-activated cyclic nucleotide-gated 1 independent grid cell-phase precession in mice. *Hippocampus* **24**, 249–256.

Erdem UM & Hasselmo M (2012). A goal-directed spatial navigation model using forward trajectory planning based on grid cells. *Eur J Neurosci* **35**, 916–931.

Erdem UM & Hasselmo ME (2014). A biologically inspired hierarchical goal directed navigation model. *J Physiol Paris* **108**, 28–37.

Erdem UM, Milford MJ & Hasselmo ME (2015). A hierarchical model of goal directed navigation selects trajectories in a visual environment. *Neurobiol Learn Mem* **117**, 109–121.

Franzius M, Sprekeler H & Wiskott L (2007). Slowness and sparseness lead to place, head-direction, and spatial-view cells. *PLoS Comput Biol* **3**, e166.

Fuhrmann F, Justus D, Sosulina L, Kaneko H, Beutel T, Friedrichs D, Schoch S, Schwarz MK, Fuhrmann M & Remy S (2015). Locomotion, theta oscillations, and the speed-correlated firing of hippocampal neurons are controlled by a medial septal glutamatergic circuit. *Neuron* **86**, 1253–1264.

Fuhs MC & Touretzky DS (2006). A spin glass model of path integration in rat medial entorhinal cortex. *J Neurosci* **26**, 4266–4276.

Fyhn M, Molden S, Witter MP, Moser EI & Moser MB (2004). Spatial representation in the entorhinal cortex. *Science* **305**, 1258–1264.

Fyhn M, Hafting T, Treves A, Moser MB & Moser EI (2007). Hippocampal remapping and grid realignment in entorhinal cortex. *Nature* **466**, 190–194.

Giocomo LM, Moser MB & Moser EI (2011). Computational models of grid cells. *Neuron* **71**, 589–603.

Glickfeld LL, Reid RC & Andermann ML (2014). A mouse model of higher visual cortical function. *Curr Opin Neurobiol* **24**, 28–33.

Graziano MS, Andersen RA & Snowden RJ (1994). Tuning of MST neurons to spiral motions. *J Neurosci* **14**, 54–67.

Guanella A, Kiper D & Verschure P (2007). A model of grid cells based on a twisted torus topology. *Int J Neural Syst* **17**, 231–240.

Hafting T, Fyhn M, Bonnevie T, Moser MB & Moser EI (2008). Hippocampus-independent phase precession in entorhinal grid cells. *Nature* **453**, 1248–1252.

Hafting T, Fyhn M, Molden S, Moser MB & Moser EI (2005). Microstructure of a spatial map in the entorhinal cortex. *Nature* **436**, 801–806.

Hardcastle K, Ganguli S & Giocomo LM (2015). Environmental boundaries as an error correction mechanism for grid cells. *Neuron* **86**, 827–839.

Hartley T, Burgess N, Lever C, Cacucci F & O'Keefe J (2000). Modelling place fields in terms of the cortical inputs to the hippocampus. *Hippocampus* **10**, 369–379.

Hasselmo ME (2008). Grid cell mechanisms and function: contributions of entorhinal persistent spiking and phase resetting. *Hippocampus* **18**, 1213–1229.

Hasselmo ME (2009). A model of episodic memory: mental time travel along encoded trajectories using grid cells. *Neurobiol Learn Mem* **92**, 559–573.

Hasselmo ME (2012). *How we Remember: Brain Mechanisms of Episodic Memory*. MIT Press, Cambridge, MA.

Hasselmo ME (2014). Neuronal rebound spiking, resonance frequency and theta cycle skipping may contribute to grid cell firing in medial entorhinal cortex. *Philos Trans R Soc Lond B Biol Sci* **369**, 20120523.

Hasselmo ME & Brandon MP (2012). A model combining oscillations and attractor dynamics for generation of grid cell firing. *Front Neural Circuits* **6**, 30.

Hasselmo ME & Shay CF (2014). Grid cell firing patterns may arise from feedback interaction between intrinsic rebound spiking and transverse traveling waves with multiple heading angles. *Front Syst Neurosci* **8**, 201.

Heys JG, Rangarajan KV & Dombeck DA (2014). The functional micro-organization of grid cells revealed by cellular-resolution imaging. *Neuron* **84**, 1079–1090.

Hinman JR, Penley SC, Long LL, Escabi MA & Chrobak JJ (2011). Septotemporal variation in dynamics of theta: speed and habituation. *J Neurophysiol* **105**, 2675–2686.

Jacobs J, Weidemann CT, Miller JF, Solway A, Burke JF, Wei XX, Suthana N, Sperling MR, Sharan AD, Fried I & Kahana MJ (2013). Direct recordings of grid-like neuronal activity in human spatial navigation. *Nat Neurosci* **16**, 1188–1190.

Jadhav SP, Kemere C, German PW & Frank LM (2012). Awake hippocampal sharp-wave ripples support spatial memory. *Science* **336**, 1454–1458.

Jeewajee A, Barry C, O'Keefe J & Burgess N (2008). Grid cells and theta as oscillatory interference: electrophysiological data from freely moving rats. *Hippocampus* **18**, 1175–1185.

Jeffery KJ, Donnett JG & O'Keefe J (1995). Medial septal control of theta-correlated unit firing in the entorhinal cortex of awake rats. *Neuroreport* **6**, 2166–2170.

Johnson A & Redish AD (2007). Neural ensembles in CA3 transiently encode paths forward of the animal at a decision point. *J Neurosci* **27**, 12176–12189.

Kemere C, Carr MF, Karlsson MP & Frank LM (2013). Rapid and continuous modulation of hippocampal network state during exploration of new places. *PLoS One* **8**, e73114.

King C, Reece M & O'Keefe J (1998). The rhythmicity of cells of the medial septum/diagonal band of Broca in the awake freely moving rat: relationships with behaviour and hippocampal theta. *Eur J Neurosci* **10**, 464–477.

Koenig J, Linder AN, Leutgeb JK & Leutgeb S (2011). The spatial periodicity of grid cells is not sustained during reduced theta oscillations. *Science* **332**, 592–595.

Kropff E, Carmichael JE, Moser MB & Moser EI (2015). Speed cells in the medial entorhinal cortex. *Nature* **523**, 419–424.

Kropff E & Treves A (2008). The emergence of grid cells: Intelligent design or just adaptation? *Hippocampus* **18**, 1256–1269.

Krupic J, Bauza M, Burton S, Barry C & O'Keefe J (2015). Grid cell symmetry is shaped by environmental geometry. *Nature* **518**, 232–235.

Krupic J, Bauza M, Burton S, Lever C & O'Keefe J (2014). How environment geometry affects grid cell symmetry and what we can learn from it. *Philos Trans R Soc Lond B Biol Sci* **369**, 20130188.

Lengyel M, Szatmary Z & Erdi P (2003). Dynamically detuned oscillations account for the coupled rate and temporal code of place cell firing. *Hippocampus* **13**, 700–714.

Lever C, Burton S, Jeewajee A, O'Keefe J & Burgess N (2009). Boundary vector cells in the subiculum of the hippocampal formation. *J Neurosci* **29**, 9771–9777.

McNaughton BL, Battaglia FP, Jensen O, Moser EI & Moser MB (2006). Path integration and the neural basis of the 'cognitive map'. *Nat Rev Neurosci* **7**, 663–678.

Mehta MR (2007). Cortico-hippocampal interaction during up-down states and memory consolidation. *Nat Neurosci* **10**, 13–15.

Mhatre H, Gorchetchnikov A & Grossberg S (2010). Grid cell hexagonal patterns formed by fast self-organized learning within entorhinal cortex. *Hippocampus* **22**, 320–334.

Milford MJ (2008). *Robot Navigation From Nature: Simulation Localization, Mapping and Path Planning Based on Hippocampal Models*. Springer, Berlin.

Milford MJ, Wiles J & Wyeth GF (2010). Solving navigational uncertainty using grid cells on robots. *PLoS Comput Biol* **6**, e1000995.

Milford MJ & Wyeth G (2010). Persistent navigation and mapping using a biologically inspired SLAM system. *Int J Robot Res* **29**, 1131–1153.

Milford MJ & Wyeth GF (2008). Mapping a suburb with a single camera using a biologically inspired SLAM system. *IEEE Trans Robot* **24**, 1038–1053.

Milner B, Corkin S & Teuber H-L (1968). Further analysis of the hippocampal amnesic syndrome: 14-year follow-up study of H.M. *Neuropsychologia* **6**, 215–234.

Mitchell SJ & Ranck JB Jr (1980). Generation of theta rhythm in medial entorhinal cortex of freely moving rats. *Brain Res* **189**, 49–66.

Mitchell SJ, Rawlins JN, Steward O & Olton DS (1982). Medial septal area lesions disrupt theta rhythm and cholinergic staining in medial entorhinal cortex and produce impaired radial arm maze behaviour in rats. *J Neurosci* **2**, 292–302.

Mizuseki K, Sirota A, Pastalkova E & Buzsaki G (2009). Theta oscillations provide temporal windows for local circuit computation in the entorhinal-hippocampal loop. *Neuron* **64**, 267–280.

Morris RG, Garrud P, Rawlins JN & O'Keefe J (1982). Place navigation impaired in rats with hippocampal lesions. *Nature* **297**, 681–683.

Moser EI & Moser MB (2008). A metric for space. *Hippocampus* **18**, 1142–1156.

Navratilova Z, Giocomo LM, Fellous JM, Hasselmo ME & McNaughton BL (2012). Phase precession and variable spatial scaling in a periodic attractor map model of medial entorhinal grid cells with realistic after-spike dynamics. *Hippocampus* **22**, 772–789.

Newman EL, Hasselmo ME (2014). Grid cell firing properties vary as a function of theta phase locking preferences in the rat medial entorhinal cortex. *Front Syst Neurosci* **8**, 193.

O'Keefe J (1976). Place units in the hippocampus of the freely moving rat. *Exp Neurol* **51**, 78–109.

O'Keefe J & Burgess N (1996). Geometric determinants of the place fields of hippocampal neurons. *Nature* **381**, 425–428.

O'Keefe J, Burgess N, Donnett JG, Jeffery KJ & Maguire EA (1998). Place cells, navigational accuracy, and the human hippocampus. *Philos Trans R Soc Lond B Biol Sci* **353**, 1333–1340.

O'Keefe J & Dostrovsky J (1971). The hippocampus as a spatial map. Preliminary evidence from unit activity in the freely-moving rat. *Brain Res* **34**, 171–175.

O'Keefe J & Nadel L (1978). *The Hippocampus as a Cognitive Map.* Oxford University Press, Oxford, UK.

O'Keefe J & Recce ML (1993). Phase relationship between hippocampal place units and the EEG theta rhythm. *Hippocampus* **3**, 317–330.

Olton DS, Becker JT & Handelmann GE (1979). Hippocampus, space and memory. *Behav Brain Sci* **2**, 313–365.

Olton DS, Wible CG & Shapiro ML (1986). Mnemonic theories of hippocampal function. *Behav Neurosci* **100**, 852–855.

Pastoll H, Solanka L, van Rossum MC & Nolan MF (2013). Feedback inhibition enables theta-nested gamma oscillations and grid firing fields. *Neuron* **77**, 141–154.

Ranck JBJ (1984). Head-direction cells in the deep cell layers of dorsal presubiculum in freely moving rats. *Soc Neurosci Abstr* **10**, 599.

Raudies F, Brandon MP, Chapman GW & Hasselmo ME (2015). Head direction is coded more strongly than movement direction in a population of entorhinal neurons. *Brain Res* 1621, 355–367.

Raudies F & Hasselmo ME (2012). Modelling boundary vector cell firing given optic flow as a cue. *PLoS Comput Biol* **8**, e1002553.

Raudies F & Hasselmo ME (2015). Differences in visual-spatial input may underlie different compression properties of firing fields for grid cell modules in medial entorhinal cortex. *PLoS Comput Biol* **11**, e1004596.

Raudies F, Mingolla E & Hasselmo ME (2012). Modelling the influence of optic flow on grid cell firing in the absence of other cues. *J Comput Neurosci* **33**, 475–493.

Rodman HR & Albright TD (1987). Coding of visual stimulus velocity in area MT of the macaque. *Vision Res* **27**, 2035–2048.

Sargolini F, Fyhn M, Hafting T, McNaughton BL, Witter MP, Moser MB & Moser EI (2006). Conjunctive representation of position, direction, and velocity in entorhinal cortex. *Science* **312**, 758–762.

Savelli F, Yoganarasimha D & Knierim JJ (2008). Influence of boundary removal on the spatial representations of the medial entorhinal cortex. *Hippocampus* **18**, 1270–1282.

Schmidt-Hieber C & Hausser M (2013). Cellular mechanisms of spatial navigation in the medial entorhinal cortex. *Nat Neurosci* **16**, 325–331.

Scoville WB & Milner B (1957). Loss of recent memory after bilateral hippocampal lesions. *J Neurol Neurosurg Pychiatry* **20**, 11–21.

Sheynikhovich D, Chavarriaga R, Strosslin T, Arleo A & Gerstner W (2009). Is there a geometric module for spatial orientation? Insights from a rodent navigation model. *Psychol Rev* **116**, 540–566.

Si B, Kropff E & Treves A (2012). Grid alignment in entorhinal cortex. *Biol Cybern* **106**, 483–506.

Skaggs WE, McNaughton BL, Wilson MA & Barnes CA (1996). Theta phase precession in hippocampal neuronal populations and the compression of temporal sequences. *Hippocampus* **6**, 149–172.

Solstad T, Boccara CN, Kropff E, Moser MB & Moser EI (2008). Representation of geometric borders in the entorhinal cortex. *Science* **322**, 1865–1868.

Stensola H, Stensola T, Solstad T, Froland K, Moser MB & Moser EI (2012). The entorhinal grid map is discretized. *Nature* **492**, 72–78.

Taube JS (1995). Head direction cells recorded in the anterior thalamic nuclei of freely moving rats. *J Neurosci* **15**, 70–86.

Taube JS & Bassett JP (2003). Persistent neural activity in head direction cells. *Cereb Cortex* **13**, 1162–1172.

Taube JS, Goodridge JP, Golob EJ, Dudchenko PA & Stackman RW (1996). Processing the head direction cell signal: a review and commentary. *Brain Res Bull* **40**, 477–484.

Taube JS, Muller RU & Ranck JB Jr (1990*a*). Head-direction cells recorded from the postsubiculum in freely moving rats. I. Description and quantitative analysis. *J Neurosci* **10**, 420–435.

Taube JS, Muller RU & Ranck JB Jr (1990*b*). Head-direction cells recorded from the postsubiculum in freely moving rats. II. Effects of environmental manipulations. *J Neurosci* **10**, 436–447.

Towse BW, Barry C, Bush D & Burgess N (2014). Optimal configurations of spatial scale for grid cell firing under noise and uncertainty. *Philos Trans R Soc Lond B Biol Sci* **369**, 20130290.

Ungerleider LG & Mishkin M (1982). Two cortical visual systems. In *Analysis of Visual Behaviour*, ed. Ingle DJ, Goodale MA, Mansfield RJW, pp. 549–586. MIT Press, Cambridge, MA.

Varga V, Hangya B, Kranitz K, Ludanyi A, Zemankovics R, Katona I, Shigemoto R, Freund TF & Borhegyi Z (2008). The presence of pacemaker HCN channels identifies theta rhythmic GABAergic neurons in the medial septum. *J Physiol* **586**, 3893–3915.

Wang Q, Gao E & Burkhalter A (2011). Gateways of ventral and dorsal streams in mouse visual cortex. *J Neurosci* **31**, 1905–1918.

Wang Q, Sporns O & Burkhalter A (2012). Network analysis of corticocortical connections reveals ventral and dorsal processing streams in mouse visual cortex. *J Neurosci* **32**, 4386–4299.

Welday AC, Shlifer IG, Bloom ML, Zhang K & Blair HT (2011). Cosine directional tuning of theta cell burst frequencies: evidence for spatial coding by oscillatory interference. *J Neurosci* **31**, 16157–16176.

Wills TJ, Barry C & Cacucci F (2012). The abrupt development of adult-like grid cell firing in the medial entorhinal cortex. *Front Neural Circuits* **6**, 21.

Zilli EA & Hasselmo ME (2010). Coupled noisy spiking neurons as velocity-controlled oscillators in a model of grid cell spatial firing. *J Neurosci* **30**, 13850–13860.

Zilli EA, Yoshida M, Tahvildari B, Giocomo LM & Hasselmo ME (2009). Evaluation of the oscillatory interference model of grid cell firing through analysis of measured period variance of some biological oscillators. *PLoS Comput Biol* **5**, e1000573.

Additional information

Competing interests

The authors have no conflict of interest.

Author contributions

M.H. and F.R. conceived simulation projects, F.R. designed and performed the simulations, and J.H. interpreted physiological data. All authors have approved the final version of the manuscript and agree to be accountable for all aspects of the work. All persons designated as authors qualify for authorship, and all those who qualify for authorship are listed.

Funding

Acknowledgements